EXPERIMENTAL CELL RESEARCH 330 (2015) 240–247

Available online at www.sciencedirect.com

ScienceDirect

journal homepage: www.elsevier.com/locate/yexcr

Research Article

Energy independent uptake and release of polystyrene nanoparticles in primary mammalian cell cultures

Ilaria Fiorentino[a], *Roberto Gualtieri*[a], *Vincenza Barbato*[a], *Valentina Mollo*[b], *Sabrina Braun*[a], *Alberto Angrisani*[a], *Mimmo Turano*[a], *Maria Furia*[a], *Paolo A. Netti*[c], *Daniela Guarnieri*[c], *Sabato Fusco*[c], *Riccardo Talevi*[a,*]

[a]*Dipartimento di Biologia, Università di Napoli "Federico II", Complesso Universitario di Monte S Angelo, Via Cinthia 80126 Napoli, Italy*

[b]*Italian Institute of Technology@CRIB Center for Advanced Biomaterials for Health Care, Largo Barsanti e Matteucci, 53, 80125 Napoli, Italy*

[c]*Dipartimento Ingegneria Chimica, dei Materiali e della Produzione Industriale -Piazzale Tecchio, 80126 Napoli, Italy*

ARTICLE INFORMATION

Article Chronology:
Received 14 June 2014
Received in revised form
10 September 2014
Accepted 11 September 2014
Available online 22 September 2014

Keywords:
Polystyrene nanoparticles
Primary cell culture
Endocytosis/exocytosis
Nanomedicine

ABSTRACT

Nanoparticle (NPs) delivery systems in vivo promises to overcome many obstacles associated with the administration of drugs, vaccines, plasmid DNA and RNA materials, making the study of their cellular uptake a central issue in nanomedicine. The uptake of NPs may be influenced by the cell culture stage and the NPs physical–chemical properties. So far, controversial data on NPs uptake have been derived owing to the heterogeneity of NPs and the general use of immortalized cancer cell lines that often behave differently from each other and from primary mammalian cell cultures.

Main aims of the present study were to investigate the uptake, endocytosis pathways, intracellular fate and release of well standardized model particles, i.e. fluorescent 44 nm polystyrene NPs (PS-NPs), on two primary mammalian cell cultures, i.e. bovine oviductal epithelial cells (BOEC) and human colon fibroblasts (HCF) by confocal microscopy and spectrofluorimetric analysis. Different drugs and conditions that inhibit specific internalization routes were used to understand the mechanisms that mediate PS-NP uptake. Our data showed that PS-NPs are rapidly internalized by both cell types 1) with similar saturation kinetics; 2) through ATP-independent processes, and 3) quickly released in the culture medium.

Our results suggest that PS-NPs are able to rapidly cross the cell membrane through passive translocation during both uptake and release, and emphasize the need to carefully design NPs for drug delivery, to ensure their selective uptake and to optimize their retainment in the targeted cells.

© 2014 Elsevier Inc. All rights reserved.

*Corresponding author. fax: +39 0679233.
E-mail address: riccardo.talevi@unina.it (R. Talevi).

http://dx.doi.org/10.1016/j.yexcr.2014.09.017
0014-4827/© 2014 Elsevier Inc. All rights reserved.

Introduction

In recent years, major efforts on nanotechnology in biomedicine have been focused on the design of nanoparticles (NPs) for targeted drug delivery, gene therapy and diagnostics. Changes in the structural and functional properties of particles (e.g., size, chemical composition, surface charge, shape and morphology) can significantly affect their interaction with cells, cell viability and blood compatibility [1–3]. As high uptake efficiency into the targeted tissue is a key goal in NP-based drug delivery systems, the study of NP selective permeability and internalization pathways has recently received growing interest. So far, the internalization mechanisms are still partially understood [3–5] due to the heterogeneity of NPs and the cell types employed.

Polystyrene NPs (PS-NPs) are widely used as a model and reference particle to study NP–cell interactions [6] both in vitro [7] and in vivo [8] for their non-immunogenic properties, low cytotoxicity and ease of size and surface modification over a broad range [9,10].

In the present paper, we chose fluorescent 44 nm PS-NPs as a model NPs to study their uptake/release kinetics, internalization pathways and subsequent intracellular fate in two primary mammalian cell cultures, to better mimic the in vivo cellular physiological response. In particular, we selected an epithelial and a connective cell type involved in secretion, endocytosis and/or barrier functions: 1) bovine oviductal epithelial cells (BOEC) that have been widely characterized, offer an excellent experimental model as they form an epithelial barrier in the female reproductive tract and are involved in the secretion of products essential for optimizing the microenvironment for oocyte maturation, sperm capacitation, fertilization, and transport of gametes and embryos [11,12]; 2) human colon fibroblasts (HCF) that synthesize the extracellular matrix and collagen of colon stroma, represent another valuable model as an attractive target for drug delivery treatments. Confocal microscopy and spectrofluorimetric analysis showed that PS-NPs are rapidly internalized and released by BOEC and HCF through passive uptake.

Materials and methods

Reagents

Medium 199 (M4530), BSA (fraction V), penicillin, streptomycin, gentamycin, amphotericin B, fetal calf serum (FCS), paraformaldehyde, sucrose, dynasore monohydrate, 5-N-Ethyl-N-IsoPropyl Amiloride (EIPA), latrunculin A, sodium azide (NaN_3), Hoechst 33342, polyvinyl alcohol (PVA), FITC-dextran, FITC-insulin, triton X 100, saponin, gelatin and trypan blue, were purchased from Sigma-Aldrich (Milan, Italy); rabbit anti-caveolin 1 from Abcam (Milan, Italy); anti-rabbit TRITC from Chemicon (Milan, Italy); Amniomed-plus ready to use medium was purchased from Euroclone (Milan, Italy); rhodamine-phalloidin was purchased from Invitrogen (Milan, Italy). Reagents and water for preparation of saline and culture media were all cell culture tested. Fluorescent green (468/508 nm) unmodified PS-NPs 44 nm in diameter was purchased from Duke Scientific Corporation (Palo Alto, California, USA).

Determination of PS-NP size, zeta potential and fluorochrome leakage

The size and zeta potential of PS-NPs were determined by dynamic light scattering (DLS). A 0.1 mg/ml suspension of PS-NPs in distilled water (12 runs each sample) was subjected to analysis using a ZetaSizer Nano ZS (Malvern Instruments, Malvern, UK). According to Salvati et al. [13], some commercial preparations of fluorescent PS-NPs have a labile fraction of fluorescent dye that is leaked from the nanoparticles and may produce artifactual results. Herein to rule out the possibility of a fluorochrome leakage from the PS-NPs, these were diluted 1/8000 in culture medium and incubated for 0, 4 and 24 h at 38.5 °C, 5% CO_2, 95% humidity. At each time point an aliquot of the suspension was filtered by centrifugation through a 10 kDa filter (15 min at 5000*g*; Amicon Ultra-0.5 ml Centrifugal Filters for Protein Purification and Concentration: Millipore, Milan, Italy) and the fluorescence intensity of the suspension, the filtrate and culture medium alone were evaluated through spectrofluorometric analysis with a Wallac 4210, Perkin-Elmer.

Cell culture

Bovine oviducts were collected at the time of slaughter and transported to the laboratory in Dulbecco's PBS (DPBS) supplemented with 50 μg/ml gentamycin at 4 °C. Laminae of epithelial cells were recovered from oviducts of single animals by squeezing and cultured in M199 supplemented with 50 μg/ml gentamycin, 1 μg/ml amphotericin B, and 10% FCS, at 38.5 °C, 5% CO_2, 95% humidity. Human colon fibroblasts (HCF) from normal colorectal mucosa, kindly gifted by Dr Marina De Rosa [14], were cultured in Amniomed-plus ready to use medium and grown at 37 °C, 5% CO_2, 95% humidity.

BOEC and HCF were initially cultured in 10 cm Petri dishes (Falcon, Becton Dickinson, Milan, Italy) for 24–48 h, and then transferred into 24-well tissue culture plates (Falcon, Becton Dickinson, Milan, Italy) with 12 mm gelatin-coated German glass round cover slips on the well bottom. Fresh media changes were performed every 48 h. Cell confluence was attained in about 7–10 days, and monolayers were used within 24 h after confluence.

Analysis of PS-NP uptake under confocal microscopy and fluorescence spectroscopy

To study PS-NP uptake, BOEC and HCF monolayers were incubated with PS-NPs in the same culture media indicated above at a final concentration of 10 μg/ml, for 1, 10, 20, 30 and 60 min. Viability was evaluated through staining with Trypan Blue 0.5%. At each time point, samples were rapidly rinsed three times in DPBS and processed for analysis under fluorescence spectroscopy and confocal microscopy.

For confocal analysis, the monolayers were fixed with 4% paraformaldehyde in PBS (PF) for 30 min, rinsed three times with PBS, treated with Hoechst 33342 10 μg/ml for 7 min and washed again. Samples were imaged using a Leica TCS SP5 equipped with Diode UV (405 nm), Argon (488 nm) and a He–Ne (543 nm) lasers with a 63 × oil immersion objective, a pinhole size of 95.5 μm, section thickness of 0.77 μm, Z-stacks of 20 μm, image resolution 1024 × 1024 pixels, and at 100 Hz. Quantitative analysis of relative fluorescence in uptake kinetics and inhibition studies was carried

out using the Leica Application Suite software (Leica Microsystems, Milan, Italy). All experiments were performed in triplicates.

For spectrofluorometric analysis the monolayers were treated with lysis buffer (Urea 7 M, Thiourea 2 M, Chaps 4%, Tris 30 mM)/DPBS 1/4 for 30 s at RT, loaded in 96-well tissue culture plates (Falcon, Becton Dickinson, Milan, Italy) and analyzed with a Wallac 4210, Perkin-Elmer.

Uptake inhibition

Different drugs and conditions that inhibit specific internalization routes, were used to understand the mechanisms of NP uptake in BOEC and HCF. To avoid triggering the activation of other endocytosis pathways by the blockage of specific uptake routes [15,16], exposure time to the inhibitors were limited to 1 h. Except for latrunculin A and 4 °C experiments, other inhibition tests were performed pre-treating the monolayers with inhibitors for 30 min and then exposing them to the NPs at a concentration of 10 μg/ml in the presence of the inhibitor for further 30 min, a time needed to achieve NP uptake saturation (see results). Cell viability was not affected by the treatments.

Hypertonic sucrose was used to inhibit clathrin-dependent endocytosis [17], dynasore to inhibit dynamin-dependent endocytosis [18], EIPA to block the Na+/H+ exchanger needed for macropinosome formation [19]. To rule out the involvement of endocytosis in PS-NP uptake, we used Latrunculin A, a drug that forms complexes with actin monomers and disrupt the organization of actin filaments [20] involved in all endocytic pathways [21]. The efficacy of Latrunculin A in actin depolymerization was evaluated through labeling with rhodamine–phalloidin before and after the treatment. To this end, monolayers were treated with latrunculin A 3 μM or medium alone for 30 and 60 min and fixed in PF. These cells were permeabilized in PBS supplemented with 1 mg/ml polyvinyl alcohol (PBS-PVA) and 0.1% Triton X 100 at 4 °C for 30 min, and treated with rhodamine–phalloidin 15UI/mL in PBS-PVA for 1 h at RT. As the maximal depolymerization of actin was attained in 1 h, inhibition experiments were performed pre-treating the monolayers with latrunculin A at 3 μM for 1 h and then as indicated but in the absence of latrunculin A. Therefore, the monolayers were pre-incubated in culture media supplemented with one of the following reagents, 0,9 mM sucrose, 80 μM dynasore, 100 μM EIPA for 30 min, or in latrunculin A, 3 μM for 1 h, and then exposed to PS-NPs.

The involvement of energy-dependent uptake was investigated by treating the monolayers at 4 °C, a temperature that inhibits all energy dependent processes [22], or with NaN_3 to inhibit ATP hydrolysis required for active transport [23]. Monolayers were pre-incubated in culture media at 4 °C for 10 min and then exposed to PS-NPs at 4 °C for 30 min. Pre-treatment with NaN_3 (0.9 mM) was performed for 30 min in DPBS and then the monolayers were incubated with PS-NPs and NaN_3 in DPBS for 30 min.

At the end of treatments, samples were rapidly rinsed three times with DPBS, assessed for viability by staining with Trypan Blue 0,5%, and analyzed by fluorescence spectroscopy and confocal microscopy as described above.

The efficiency of inhibitory treatments was evaluated incubating the monolayers for 1 h with 100 μg/ml FITC-insulin or 5 mg/ml FITC-dextran.

Localization of caveolin 1

The possible involvement of caveolin-dependent endocytosis in NPs uptake was further analyzed through immunofluorescence co-localization studies. Monolayers were incubated with 10 μg/ml PS-NPs for 30 min, rinsed three times in DPBS, fixed in PF for 30 min at RT and rinsed again. Samples were then treated with 50 mM ammonium chloride in PBS 2 × 10 min, permeabilized with 0.75% saponin and 0.2% gelatin in PBS for 20 min at RT, incubated with 1:200 rabbit anti-caveolin 1 overnight at 4 °C under agitation, rinsed as above, incubated with anti-rabbit TRITC 1:100 in PBS supplemented with 0.5% BSA for 1 h at RT. Samples were then rinsed three times with PBS, and stained with Hoechst 33,342 10 μg/ml for 7 min at RT.

Imaging of labeled samples was performed on the CLSM with the 488 nm argon laser, 543 nm He–Ne laser and a 63 × oil immersion objective.

PS-NP release

To understand whether NPs were retained within the cells following their internalization, CLSM and quantitative fluorescence spectroscopy experiments were performed. To this end, monolayers were incubated in 10 μg/ml PS-NPs until saturation, rinsed three times with fresh medium and incubated in fresh culture media. At 0, 1, 10, 30, 60, 120, 180 and 240 min monolayers were rapidly rinsed three times with DPBS and treated for spectrofluorometric and confocal analysis as described above. At the end of treatments, viability was evaluated through Trypan Blue staining.

Statistical analysis

The data are presented as mean ± standard deviation (SD). Overall analysis was performed by the estimate model of analysis of variance (ANOVA) followed by the Tukey's honestly significant difference test for pair wise comparisons when overall significance was detected. Percentage data were compared by χ^2 or Fisher's exact test.

Results

Determination of PS-NP size, zeta potential and fluorochrome leakage

The analysis by dynamic laser light scattering showed a NPs size of 43.67 ± 1.08 nm in diameter, with a value of 0.09 polydispersity index (PDI) and a ζ potential of −25.25 ± 5.26 mV. Spectrofluorometric analysis of PS-NP suspensions in culture medium and of the corresponding filtrates at 0, 4 and 24 h of incubation demonstrated that the fluorescence of the suspensions (arbitrary fluorescence units at 0, 4, 24 h: 348 ± 12, 326 ± 20, 305 ± 14) was stable over time whereas the fluorescence intensity of the filtrates (0, 4, 24 h: 140 ± 16, 134 ± 8, 129 ± 7) was nearly identical to that of medium alone (mean 152 ± 7) throughout the analysis thus demonstrating a lack of dye leakage from PS-NPs.

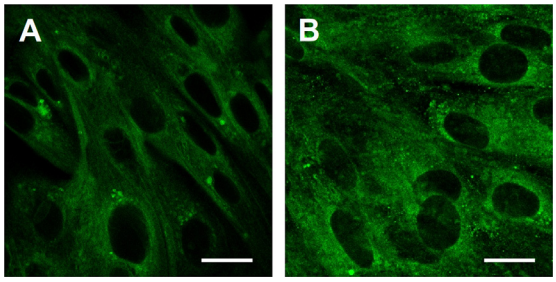

Fig. 1 – PS-NP uptake. Representative confocal micrographs of FITC conjugated PS-NPs internalized in BOEC (A) and HCF (B) after 30 min of incubation. Bar, 20 μm.

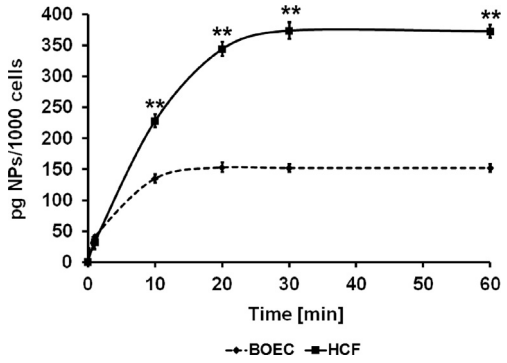

Fig. 2 – PS-NP uptake. Spectrofluorimetric analysis of PS-NP uptake in BOEC (dashed line) and HCF (solid line). **, BOEC vs HCF $P<0.01$.

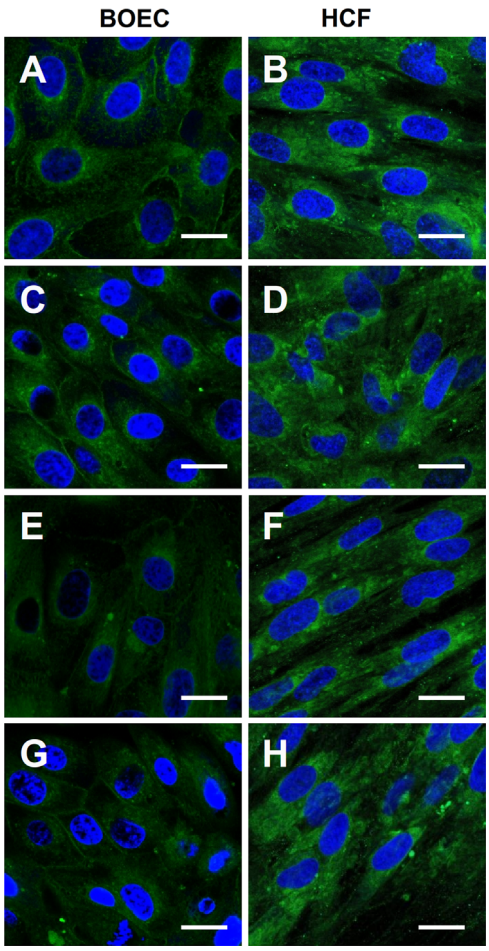

Fig. 3 – PS-NP uptake inhibition. Effects of sucrose (C and D), dynasore (E and F), and EIPA (G and H) on PS-NP uptake in BOEC and HCF compared to controls (A and B). PS-NPs, green; Nuclei, blue. Bar, 20 μm.(For interpretation of the references to color in this figure legend, the reader is referred to the web version of this article.)

PS-NP uptake

Confocal analysis showed an efficient internalization of PS-NPs both in BOEC and HCF. The PS-NPs were mostly diffused in the cytoplasm and also localized in small discrete clusters in the perinuclear region, but absent in the nucleus in both cell types (Fig. 1A and B). The fluorescent signal was clearly detectable at 1 min of incubation and continued to increase at 10 min reaching a plateau at 20–30 min. Quantitative spectrofluorimetric analysis (Fig. 2A and B; values expressed as pg NPs/1000cells) confirmed a significant uptake of PS-NPs starting at 1 min of incubation (BOEC 40,4±2.02; HCF 31,8±11,4; $P>0.05$) that exponentially increased during the first 10 min in BOEC (135±6.77) and 20 min in HCF (344±11.5) reaching a plateau after 20 min in BOEC (153±6.35) and 30 min in HCF (374±13.8) (BOEC vs HCF at 10–60 min, $P<0.01$). Viability at the end of treatments was ≥95% demonstrating the lack of cytotoxicity of the NPs.

Uptake inhibition

Specific drugs that inhibit different internalization pathways were used to understand the specific mechanisms of PS-NP uptake.

Fig. 3A and B respectively show the BOEC and HCF controls of uptake inhibition studies carried out with hypertonic sucrose, dynasore, EIPA and latrunculin A using CLSM. Data analysis demonstrated that hypertonic sucrose (Fig. 3C and D) and dynasore (Fig. 3E and F), that respectively inhibit clathrin-dependent and dynamin-dependent endocytosis, had no effects on NP uptake. EIPA (Fig. 3G and H), a specific inhibitor of macropinocytosis, also had no effects on uptake both in BOEC and HCF. The possible role of caveolin-dependent endocytosis in PS-NP uptake was also excluded by CLSM analysis of PS-NPs and caveolin 1 co-localization (Fig. 4). Latrunculin A, that disrupts the organization of actin filaments involved in all endocytic pathways [21], did not inhibit PS-NP uptake (Fig. 5 A and B). Labeling with rhodamine–phalloidin before (Fig. 5C and D) and after treatment with latrunculin A (Fig. 5E and F) clearly demonstrated the efficiency of the treatment on actin depolymerization. Quantitative spectrofluorometric analysis (Fig. 6) confirmed that none of the inhibitors affected PS-NP uptake.

Alternative methods used in the present study to inhibit active uptake were to cool cells to 4 °C or to treat them with NaN_3. The incubation at 4 °C showed a moderate inhibition of PS-NP internalization at the CLSM level in BOEC (Fig. 7C), but not in HCF (Fig. 7D) compared to respective controls (Fig. 7A and B). Quantitative spectrofluorometric analysis (Fig. 8) confirmed an inhibition of about 40% in BOEC ($P<0,01$). Finally, the incubation with NaN_3, that blocks ATP hydrolysis, did not influence the uptake in both cell types (Figs. 7G and H; 8). Positive cont-

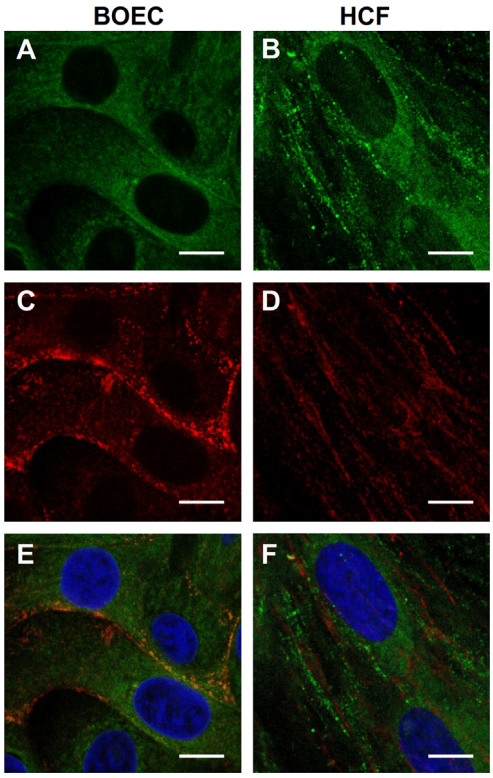

Fig. 4 – Caveolin PS-NP co-localization. FITC conjugated PS-NPs (green) and anti caveolin 1 (red) in BOEC and HCF. A and B) green channel; C and D) red channel; E and F) merge. Nuclei were counterstained with Hoechst 33342 (blue). Bar, 10 μm. (For interpretation of the references to color in this figure legend, the reader is referred to the web version of this article.)

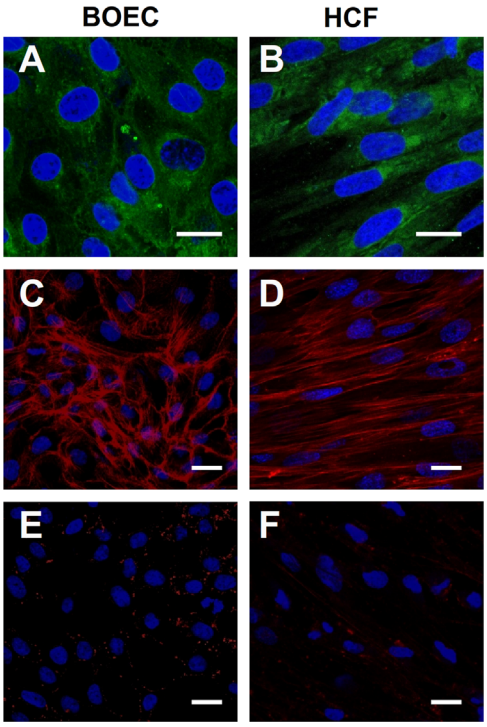

Fig. 5 – Effects of microfilament disruption on PS-NP uptake. Effect of latrunculin A on PS-NP uptake (green) in BOEC (A) and HCF (B) (see respective controls in Fig. 3 A and B). Localization of actin filaments through rhodamine-phalloidin (C–F, red) in BOEC (C and E) and HCF (D and F) before (C and D) and after latrunculin A treatment (E and F) demonstrate the efficacy of the drug in the disruption of microfilaments. Nuclei were counterstained with Hoechst 33342 (blue). Bar, 20 μm. (For interpretation of the references to color in this figure legend, the reader is referred to the web version of this article.)

rol experiments revealed a significant inhibition of FITC-insulin and FITC-dextran internalization in all treatments and in both cell types.

Viability at the end of treatment was ≥95% demonstrating the lack of cytotoxicity of the inhibition drugs and treatments used.

PS-NP release

The CLSM (Fig. 9) and spectrofluorometric (Fig. 10) analyses showed that the internalized PS-NPs are quickly released upon incubation in fresh medium. Data (Fig. 10, values as pg NPs/1000cells) revealed a sudden and significant release of NPs (time 0: BOEC,161±5,2; HCF, 360±14,8, $P<0.01$) at 1 min of incubation in fresh medium that reached 60% in BOEC (64,4±8,22) and 44% in HCF (203±10,8). The release of NPs continued with a different kinetics in BOEC and HCF and it achieved 90% at 10 min in HCF (25,6±10,1) and 180 min in BOEC (14,6±3,2). (BOEC vs HCF at 0–60 min, $P<0.01$; BOEC vs HCF at 120 min, $P<0.05$)

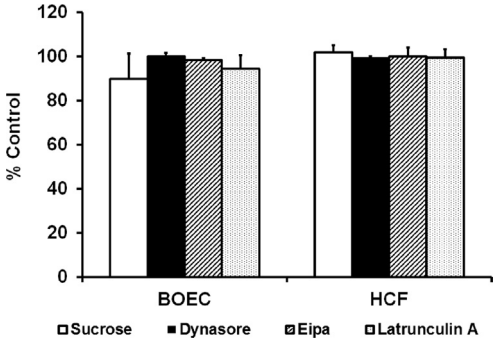

Fig. 6 – PS-NP uptake inhibition. Spectrofluorimetric analysis of the effects of sucrose, dynasore, EIPA and latrunculin A on PS-NP uptake in BOEC and HCF.

Discussion

The interactions of NPs with cells are modulated by their physicochemical properties such as size, shape, surface charge and chemistry and by cell-specific features. The comprehension of the NP-cell interaction is needed to control the NP selective targeting and uptake in biomedical applications [3,4,24]. Controversial results emphasize the need for further research to fully understand the NP internalization mechanisms [3–5].

Main aims of the present study were to investigate the behavior of PS-NPs, as model particles, in two primary cell cultures, BOEC and HCF, with different embryological origin, functions and fate.

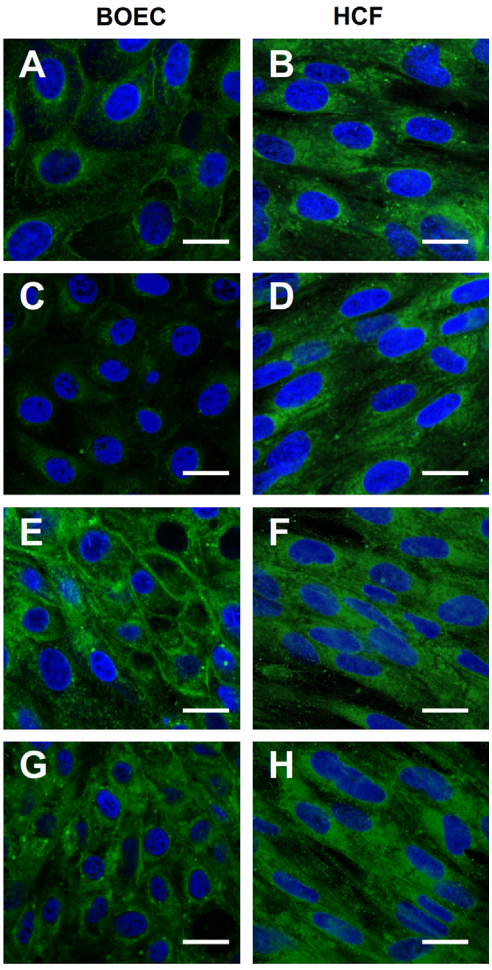

Fig. 7 – PS-NP uptake inhibition. Effects of cooling to 4 °C (controls, A and B; treated, C and D) and of sodium azide (controls, E and F; treated, G and H) on PS-NP uptake in BOEC (A,C,E and G) and HCF (B,D,F and H). PS-NPs, green; Nuclei, blue. Bar, 20 μm.(For interpretation of the references to color in this figure legend, the reader is referred to the web version of this article.)

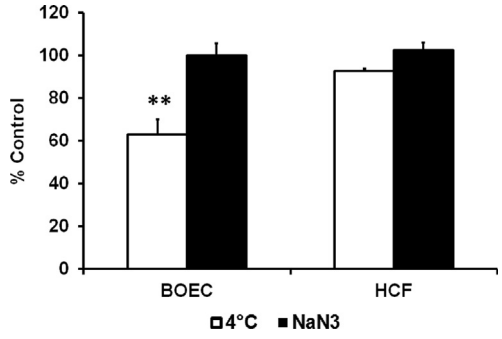

Fig. 8 – PS-NP uptake inhibition. Spectrofluorimetric analysis of the effects of cooling to 4 °C and of sodium azide on PS-NP uptake in BOEC and HCF. **, treatment vs control, $P<0.01$.

Data showed that PS-NPs are rapidly internalized by BOEC and HCF 1) with similar saturation kinetics; 2) through passive uptake processes, and 3) rapidly released in the culture medium.

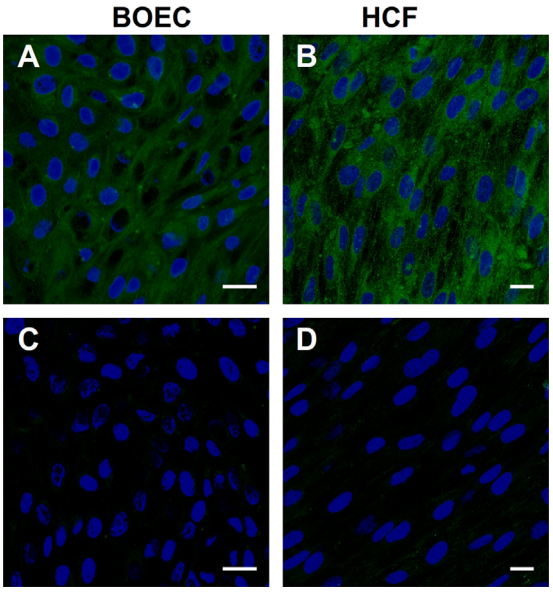

Fig. 9 – PS-NP release upon incubation in fresh culture medium. BOEC (A and C) and HCF (B and D) were incubated with PS-NPs for 30 min (A and B) and then washed and incubated in fresh medium for 180 min (C and BOEC) or 10 min (D and HCF). PS-NPs, green; Nuclei, blue. Bar, 20 μm.(For interpretation of the references to color in this figure legend, the reader is referred to the web version of this article.)

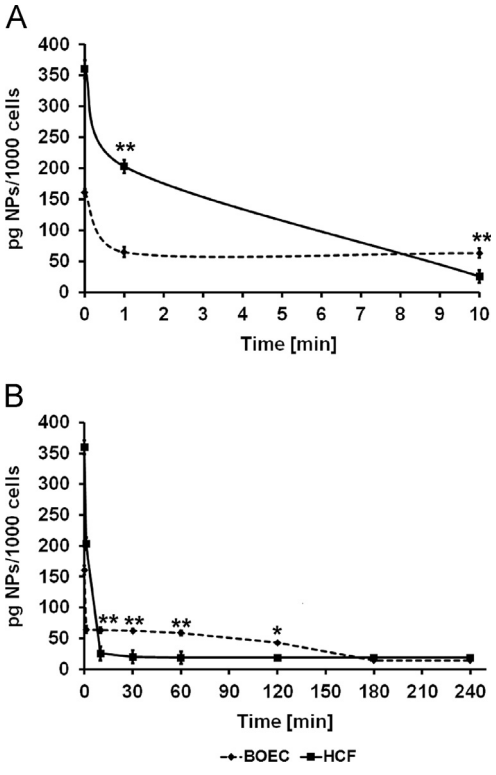

Fig. 10 – Spectrofluorimetric analysis of PS-NP release kinetics during the incubation in fresh culture medium. BOEC (dashed line) and HCF (solid line) incubated in fresh medium for 10 (A) or 240 min (B). *, BOEC vs HCF $P<0.05$. **, BOEC vs HCF $P<0.01$.

PS-NPs were efficiently internalized by both cell types. They were mostly diffused in the cytoplasm and also localized in small discrete clusters in the perinuclear region, but absent in the nucleus. The presence of a diffuse cytoplasmic signal and small NP clusters could suggest the co-existence of endocytic and non endocytic mechanisms of uptake. A similar cytoplasmic distribution and the existence of mechanisms that promote the nuclear exclusion of plain, carboxylated or amine-modified PS-NPs, with size ranging from 20 to 100 nm, have been reported in several recent studies [25–29].

Until now, studies dealing with PS-NP internalization kinetics are few and results are often discordant. PS-NP uptake kinetics and saturation were reported to range from seconds [4] to hours [25,30]. A rapid kinetics of PS-NP uptake, similar to that detected herein, was reported in a variety of cell lines and primary cell cultures interacting with plain, carboxylated or amine-modified PS-NPs of similar size [25,26,29]. The kinetics of PS-NP uptake is known to be affected by their size and charge where hydrophobic and positively charged PS-NPs show faster uptake kinetics compared to negatively charged PS-NPs [26,31]. In the present study, the negative zeta potential of plain PS-NPs is likely to be due to the presence of a stabilizing anionic surfactant and the uptake kinetics was comparable to that shown for carboxylated PS-NPs in primary rat alveolar epithelial cell and Madin Darby canine kidney cell II monolayers [26,31]. As described above, PS-NPs were detectable inside BOEC and HCF from the first minute of incubation and achieved a plateau condition at 20–30 min. However, the selected cell type can strongly affect the uptake kinetics. In fact, when the same plain PS-NPs used herein were tested on porcine aortic endothelial cells they were rapidly internalized but the achievement of a plateau was attained only after several hours [30].

A further fundamental, but also controversial issue in the cell–NP interaction is represented by the uptake mechanisms that can be affected by both the cell type and the NP structural/functional properties [3,32,33]. The identification of specific internalization mechanisms of NPs in cells is highly complex and still not fully understood [3–5]. To this end, we performed a series of uptake inhibition studies with drugs and conditions that interfere with single or multiple energy dependent internalization pathways. Our data showed no significant inhibition of NP uptake in both cell types upon blockage of 1) clathrin-dependent endocytosis through sucrose, 2) clathrin and caveolin-dependent endocytosis through dynasore, and 3) macropinocytosis through EIPA. This is in agreement with several studies showing that PS-NPs were internalized mainly via clathrin-independent endocytosis in human mesenchymal stem cells [25], in porcine aortic endothelial cells [30], and in HeLa cells [15,34]. Other studies ruled out the involvement of macropinocytosis in the uptake of negatively charged PS-NPs in HeLa cells [15] and of both macropinocytosis and dynamin-dependent endocytosis in the uptake of positively and negatively charged PS-NPs in rat alveolar epithelial monolayers [26]. Again it should be stressed that the routes of uptake are dependent on the specific cell type utilized. In fact, positively charged PS-NPs traverse rat alveolar epithelial monolayers through non endocytic mechanisms [26], and MDCK-II cells in an energy dependent manner [31].

To exclude the involvement of other energy dependent mechanisms in PS-NP uptake we analyzed the effects of the microfilament disruption by latrunculin A, cooling to 4 °C, and inhibition of ATP hydrolysis by sodium azide. Findings showed that all treatments failed to inhibit PS-NP uptake, suggesting that PS-NPs enter BOEC and HCF passively. A mechanism of passive translocation through the cell membrane was unequivocally demonstrated in red blood cells that are not endowed with the endocytic machinery [35]. Moreover, PS-NP uptake in several other cell types were demonstrated to proceed through a complete [26,31] or partial involvement of passive mechanisms [29,30]. Interestingly, Salvati et al. [13] demonstrated that a variable amount of labile dye was present in all PS-NP preparations tested therein and could be responsible for artifactual evidences of energy independent translocation. Herein, spectrofluorometric analysis of PS-NP suspensions in culture medium and of the corresponding filtrates at 0, 4 and 24 h of incubation unequivocally demonstrated the lack of dye leakage from our PS-NP preparation. Moreover, this is not the first report that clearly demonstrates that PS-NPs can be internalized through passive translocation in some cell types. In fact, the same preparation of positively charged PS-NPs entered primary rat alveolar epithelial cell and Madin Darby canine kidney cell II monolayers through passive and active uptake respectively, whereas negatively charged PS-NPs were internalized passively in both cell types [26,31]. Passive translocation of PS-NPs may involve a transient permeabilization according to the cell type [26,29]. As under our experimental conditions, the cell impermeant dye trypan blue did not penetrate the cells exposed to PS-NPs, it is likely that the uptake did not involve a permeabilization of the cell membrane but occurred through passive translocation. A further crucial and still unresolved issue in literature concerns the action of the surfactant that can adsorb to the NPs surface and affect their mode of uptake. We cannot rule out the possibility that the chemical properties of the surfactant could affect the uptake of PS-NPs. Such a fundamental issue warrants further specific studies.

We showed that the internalized PS-NPs were released according to a rapid kinetics, about 50% being lost at 1 min of incubation in fresh medium. This finding further supports the view that uptake of PS-NPs in BOEC and HCF proceeds through passive non endocytic mechanisms. Indeed, the release from BOEC and HCF monolayers cultured on a solid surface could be analogous to the non-endocytic transcellular flux of PS-NPs observed in rat alveolar epithelial and MDCK-II monolayers cultured on filter inserts [26,31].

To conclude, the present study identified the mechanisms of PS-NP uptake in an epithelial barrier and a connective cell type thus contributing to the correlation of uptake behavior and NP properties. However, given the wide variety of NPs and biomedically relevant cell types, the influence of physical and chemical properties of NPs on cell-specific routes of uptake still deserves further attention. Taken together our data emphasizes the need to carefully control the design of NPs for drug delivery, to ensure their selective uptake and optimize their retainment in the targeted cells.

Acknowledgments

This work was supported by the University of Naples Federico II and by P.O.R. Campania FSE 2007-2013, Project CREMe. Alberto Angrisani, Ilaria Fiorentino and Vincenza Barbato were awarded a

postdoctoral fellowship by P.O.R. Campania FSE 2007-2013, Project CREMe.

REFERENCES

[1] J.W. Yoo, N. Doshi, S. Mitragotri, Endocytosis and intracellular distribution of PLGA particles in endothelial cells: effect of particle geometry, Macromol. Rapid Commun. 31 (2010) 142–148.

[2] P. Decuzzi, B. Godin, T. Tanaka, S.Y. Lee, C. Chiappini, X. Liu, M. Ferrari, Size and shape effects in the biodistribution of intravascularly injected particles, J. Control Release 141 (2010) 320–327.

[3] K. Saha, S.T. Kim, B. Yan, O.R. Miranda, F.S. Alfonso, D. Shlosman, V.M. Rotello, Surface functionality of nanoparticles determines cellular uptake mechanisms in mammalian cells, Small 9 (2013) 300–305.

[4] P.H. Hemmerich, A.H. von Mikecz, Defining the subcellular interface of nanoparticles by live-cell imaging, PLoS One 8 (2013) e62018.

[5] J. Voigt, J. Christensen, V.P. Shastri, Differential uptake of nanoparticles by endothelial cells through polyelectrolytes with affinity for caveolae, Proc. Natl. Acad. Sci. USA 111 (2014) 2942–2947.

[6] J.A. Varela, M.G. Bexiga, C. Åberg, J.C. Simpson, K.A. Dawson, Quantifying size-dependent interactions between fluorescently labeled polystyrene nanoparticles and mammalian cells, J. Nanobiotechnology 10 (2012) 39.

[7] I. Papageorgiou, C. Brown, R. Schins, S. Singh, R. Newson, S. Davis, J. Fisher, E. Ingham, C.P. Case, The effect of nano- and micron-sized particles of cobalt-chromium alloy on human fibroblasts in vitro, Biomaterials 28 (2007) 2946–2958.

[8] N.R. Yacobi, L. Demaio, J. Xie, S.F. Hamm-Alvarez, Z. Borok, K.J. Kim, E.D. Crandall, Polystyrene nanoparticle trafficking across alveolar epithelium, Nanomedicine 4 (2008) 139–145.

[9] W. Zauner, N.A. Farrow, A.M.R. Haines, In vitro uptake of polystyrene microspheres: effect of particle size, cell line and cell density, J. Control Release 71 (2001) 39–51.

[10] K.Y. Win, S.S. Feng, Effects of particle size and surface coating on cellular uptake of polymeric nanoparticles for oral delivery of anticancer drugs, Biomaterials 26 (2005) 2713–2722.

[11] S.S. Suarez, Formation of a reservoir of sperm in the oviduct, Reprod. Domest. Anim. 37 (2002) 140–143.

[12] R. Talevi, R. Gualtieri, In vivo versus in vitro fertilization, Eur. J. Obstet. Gynecol. Reprod. Biol. 115 (Suppl 1) (2004) S68–S71.

[13] A. Salvati, C. Aberg, T. dos Santos, J. Varela, P. Pinto, I. Lynch, K.A. Dawson, Experimental and theoretical comparison of intracellular import of polymeric nanoparticles and small molecules: toward models of uptake kinetics, Nanomedicine 7 (2011) 818–826.

[14] M. Galatola, E. Miele, C. Strisciuglio, L. Paparo, D. Rega, P. Delrio, F. Duraturo, M. Martinelli, G.B. Rossi, A. Staiano, P. Izzo, M. De Rosa, Synergistic effect of interleukin-10-receptor variants in a case of early-onset ulcerative colitis, World J. Gastroenterol. 19 (2013) 8659–8670.

[15] J. Dausend, A. Musyanovych, M. Dass, P. Walther, H. Schrezenmeier, K. Landfester, V. Mailänder, Uptake mechanism of oppositely charged fluorescent nanoparticles in HeLa cells, Macromol. Biosci. 8 (2008) 1135–1143.

[16] H.J. Johnston, M. Semmler-Behnke, D.M. Brown, W. Kreyling, L. Tran, V. Stone, Evaluating the uptake and intracellular fate of polystirene nanoparticles by primary and hepatocyte cell lines in vitro, Toxicol. Appl. Pharmacol. 242 (2010) 66–78.

[17] M.G. Qaddoumi, H.J. Gukasyan, J. Davda, V. Labhasetwar, K.J. Kim, V.H. Lee, Clathrin and caveolin-1 expression in primary pigmented rabbit conjunctival epithelial cells: role in PLGA nanoparticle endocytosis, Mol. Vis. 9 (2003) 559–568.

[18] T. Kirchhausen, E. Macia, H.E. Pelish, Use of dynasore, the small molecule inihibtor of dynamin, in the regulation of endocytosis, Methods Enzymol. 438 (2008) 77–93.

[19] J. Mercer, A. Helenius, Vaccinia virus uses macropinocytosis and apoptotic mimicry to enter host cells, Science 320 (2008) 531–535.

[20] W.M. Morton, K.R. Ayscough, P.J. McLaughlin, Latrunculin alters the actin-monomer subunit interface to prevent polymerization, Nat. Cell Biol. 2 (2000) 376–378.

[21] B. Qualmann, M.M. Kessels, R.B. Kelly, Molecular links between endocytosis and the actin cytoskeleton, J. Cell Biol. 150 (2000) F111–F116.

[22] A. Verma, O. Uzun, Y. Hu, Y. Hu, H.S. Han, N. Watson, S. Chen, D.J. Irvine, F. Stellacci, Surface-structure-regulated cell-membrane penetration by monolayer-protected nanoparticles, Nat. Mater. 7 (2008) 588–595.

[23] E.A. Vasilyeva, M.J. Forgac, Interaction of the clathrin-coated vesicle V-ATPase with ADP and sodium azide, Biol. Chem. 273 (1998) 23823–23829.

[24] G. Sahay, D.Y. Alakhova, A.V. Kabanov, Endocytosis of nanomedicines, J. Contro 145 (2010) 182–195.

[25] X. Jiang, J. Dausend, M. Hafner, A. Musyanovych, C. Röcker, K. Landfester, V. Mailänder, G.U. Nienhaus, Specific effects of surface amines on polystyrene nanoparticles in their interactions with mesenchymal stem cells, Biomacromolecules 11 (2010) 748–753.

[26] N.R. Yacobi, N. Malmstadt, F. Fazlollahi, L. DeMaio, R. Marchelletta, S.F. Hamm-Alvarez, Z. Borok, K.J. Kim, E.D. Crandall, Mechanisms of alveolar epithelial translocation of a defined population of nanoparticles, Am. J. Respir. Cell Mol. Biol. 42 (2010) 604–614.

[27] Y. Liu, W. Li, F. Lao, Y. Liu, L. Wang, R. Bai, Y. Zhao, C. Chen, Intracellular dynamics of cationic and anionic polystyrene nanoparticles without direct interaction with mitotic spindle and chromosomes, Biomaterials 32 (2011) 8291–8303.

[28] J.D. Larsen, N.L. Ross, M.O. Sullivan, Requirements for the nuclear entry of polyplexes and nanoparticles during mitosis, J. Gene Med. 14 (2012) 580–589.

[29] P.J. Smith, M. Giroud, H.L. Wiggins, F. Gower, J.A. Thorley, B. Stolpe, J. Mazzolini, R.J. Dyson, J.Z. Rappoport, Cellular entry of nanoparticles via serum sensitive clathrin-mediated endocytosis, and plasma membrane permeabilization, Int. J. Nanomed. 7 (2012) 2045–2055.

[30] D. Guarnieri, A. Guaccio, S. Fusco, P.A. Netti, Effect of serum proteins on polystyrene nanoparticle uptake and intracellular trafficking in endothelial cells, J Nanoparticle Res. 13 (2011) 4295–4309.

[31] F. Fazlollahi, S. Angelow, N.R. Yacobi, R. Marchelletta, A.S. Yu, S.F. Hamm-Alvarez, Z. Borok, K.J. Kim, E.D. Crandall, Polystyrene nanoparticle trafficking across MDCK-II, Nanomedicine 7 (2011) 588–594.

[32] D.F. Moyano, V.M. Rotello, Nano meets biology: structure and function at the nanoparticle interface, Langmuir 27 (2011) 10376–10385.

[33] W.J. Stark, Nanoparticles in biological systems, Angew. Chem. Int. Ed. Engl. 50 (2011) 1242–1258.

[34] S. Lerch, M. Dass, A. Musyanovych, K. Landfester, V. Mailänder, Polymeric nanoparticles of different sizes overcome the cell membrane barrier, Eur J Pharm Biopharm. 84 (2013) 265–274.

[35] B.M. Rothen-Rutishauser, S. Schurch, B. Haenni, N. Kapp, P. Gehr, Interaction of fine particles and nanoparticles with red blood cells visualized with advanced microscopic techniques, Environ Sci. Technol. 40 (2006) 4353–4359.